PHYSICS AND CHEMISTRY
OF SOLID STATE
V. 26, No.3 (2025) pp. 592-597

Section: Chemistry

DOI: 10.15330/pcss.26.3.592-597

Vasyl Stefanyk Carpathian
National University

ФІЗИКА І ХІМІЯ ТВЕРДОГО ТІЛА
Т. 26, № 3 (2025) С. 592-597

Хімічні науки

UDC: 546.882

ISSN 1729-4428 (Print)
ISSN 2309-8589 (Online)

L. Romaka[1], Yu. Stadnyk[1], V.V. Romaka[2,3], Yu. Yatskiv[1], M. Konyk[1]

Isothermal section of the Dy-Cr-Ge system at 1073 K

[1]*Ivan Franko National University of Lviv, Lviv, Ukraine, lyubov.romaka@gmail.com*
[2]*Technische Universität Dresden, Chair of Inorganic Chemistry II, Dresden, Germany, vitaliy.romaka@tu-dresden.de*
[3]*Institute for Solid State Research, IFW-Dresden, Dresden, Germany*

The phase equilibrium diagram of the Dy–Cr–Ge ternary system was constructed over the whole concentration range at 1073 K using methods of powder X-ray diffractometry, metallography, and electron microprobe analysis. Three ternary compounds are formed in the Dy-Cr-Ge system at the annealing temperature: $Dy_{117}Cr_{52}Ge_{112}$ ($Tb_{117}Fe_{52}Ge_{112}$ structure type, space group *Fm*-3*m*, $a = 2.8723(8)$ nm), $DyCr_6Ge_6$ ($SmMn_6Sn_6$ structure type, space group *P*6/*mmm*, $a = 0.51642(1)$, $c = 0.82767(2)$ nm), $DyCr_{1-x}Ge_2$ ($CeNiSi_2$ structure type, space group *Cmcm*, $a = 0.41249(5)$-$0.4140(3)$, $b = 1.58287(2)$-$1.5890(7)$, $c = 0.40048(5)$-$0.4001(2)$ nm). The $DyCr_{1-x}Ge_2$ compound with $CeNiSi_2$ structure type is characterized by a small homogeneity range limited by the $DyCr_{0.28}Ge_2$ and $DyCr_{0.30}Ge_2$ compositions. The solubility of chromium in the binary germanide Dy_5Ge_3 (Mn_5Si_3-type) extends up to 4 at. %. The DFT calculations were used to evaluate the thermodynamic, elastic and electrical properties of the $DyCr_{1-x}Ge_2$ compound.

Keywords: Intermetallics; X-ray diffraction, phase equilibria, crystal structure.

Received 07 November 2024; Accepted 16 September 2025.

Introduction

The investigation of phase equilibria of the Dy−Cr−Ge system is part of a systematic study of the interaction between the components in ternary systems based on rare earth metals with 3*d*-elements and germanium to find new intermetallic compounds and study their physical properties To better understand the physical properties of intermetallics, the important step is to determine their relation of equilibrium with other phases and peculiarities of the crystal structure.

Among the ternary systems R−Cr−Ge (R is a rare earth metal), phase equilibrium diagrams are studied for R = Nd, Y, Gd, Er, and Tm [1-5]. Analysis of the literature data shows that the most studied compounds are $RCr_{1-x}Ge_2$ ($CeNiSi_2$-type) [6], RCr_6Ge_6 ($SmMn_6Sn_6$-type) [7], and $RCrGe_3$ ($BaNiO_3$-type) [8]. $RCrGe_3$ germanides (R = La-Nd, Sm) are characterized by ferromagnetic behavior with high Curie temperatures ranging from 60 to 155 K [8]. Detailed structural study of the RCr_6Ge_6 compounds (R=Gd, Dy-Lu) shows that all studied compounds revealed the off-stoichiometric composition [7]. Magnetic property measurements of RCr_6Ge_6 germanides found magnetic ordering on $TbCr_6Ge_6$, $DyCr_6Ge_6$, and $ErCr_6Ge_6$ [9, 10], $TmCr_6Ge_6$ and $LuCr_6Ge_6$ are paramagnets down to 2 K [7]. $YbCr_6Ge_6$ germanide exhibits a magnetic transition at 3.4 K [7] with the ferrimagnetic ordering of the Cr and Yb sublattices. $R_{117}Cr_{52}Ge_{112}$ compounds with a giant unit cell ($Tb_{117}Fe_{52}Ge_{112}$-type, $a \sim 2.9$ nm) were found with R= Nd, Sm, and Gd [11, 12, 4]. The complexity of their crystal structure, which provides low thermal conductivity, is a basis for the creation of promising thermomagnetic materials.

In this contribution, we present experimental results from a study of the interaction between the components in the Dy-Cr-Ge system at 1073 K.

I. Experimental methods

To construct the phase equilibrium diagram of the Dy-Cr-Ge system polycrystalline samples were synthesized by a direct arc-melting of the constituent components (metals were used in the form of ingots, with purity of dysprosium 99.9 wt.%; chromium, purity of 99.99 wt.%; and germanium, purity of 99.999 wt.%) under protected argon atmosphere (high purity Ti-gettered) on a water-cooled copper bottom. The alloys were re-melted twice to provide better homogenization. The weight loss of the samples during the synthesis was less than 1 % of the initial total mass. Heat treatment of the produced alloys was performed in vacuum quartz ampoules at a temperature of 1073 K for 700 h. Then, the alloys were quenched in cold water without breaking the ampoules. The annealed samples were examined by X-ray diffractometry (DRON-4.0 diffractometer, Fe*K*α radiation) to determine the phase composition. The observed diffraction intensities were compared with reference powder patterns of the binary phases, known ternary germanides, and pure elements (program PowderCell [13]). To control the chemical composition of the synthesized samples, determine the exact content of components in the phases, and confirm the phase composition, the method of energy-dispersive X-ray spectroscopy (EDRS) (electron microscope TESKAN VEGA 3 LMU, equipped by an X-ray analyzer with energy dispersive spectroscopy) was used. At least five measurements were taken to obtain the average value for each phase in each sample. For the crystal structure refinement, the diffraction data were collected at room temperature using STOE STADI P diffractometer (graphite monochromator, Cu $K\alpha_1$ radiation). Rietveld refinement of the crystal structure was performed using the FullProf Suite program package [14].

The DFT calculations were performed using Vienna Ab initio Simulation Package VASP v.5.4.4 with PAW-type potentials [15]. The Perdew-Burke-Enzerhoff (PBE) exchange-correlation functional in the generalized gradient approximation (GGA) [16] with an 11×11×11 Monkhorst-Pack *k*-point set [17] was used in both cases. The semi-core 4*f*-electrons of Dy atoms were treated as core states. Optimized crystal structures were used for the final total energy calculations. Complete geometry relaxation (atomic positions and lattice parameters) was achieved by minimizing forces, stress tensor components, and total energies. The Bader charge density analysis was performed using the Bader v1.05 code [18].

II. Experimental results

2.1. Isothermal section of the Dy-Cr-Ge system

The data concerning the binary boundary Dy–Ge, Cr–Ge, and Dy–Cr systems were taken from the reported phase diagrams [19, 20]. No binary phases are formed in the Dy–Cr system. In the Cr–Ge system, four binary phases were confirmed at the temperature of annealing: $Cr_{11}Ge_{19}$ ($Mn_{11}Si_{19}$-type), CrGe (FeSi-type), $Cr_{11}Ge_8$ ($Cr_{11}Ge_8$-type), and Cr_3Ge (Cr_3Si-type). The Cr_5Ge_3 binary with W_5Si_3 structure type was not identified at the investigation temperature. According to the performed phase analysis, the sample at the corresponding composition contains two binary phases, Cr_3Ge and $Cr_{11}Ge_8$, in equilibrium. As reported in the literature Cr_5Ge_3 binary is stable at higher temperature, formed by peritectic reaction at 1535 K and decomposes under the eutectoid reaction at 1269 K. Nine binary compounds were confirmed in the Dy-Ge system at 1073 K: $DyGe_3$ ($DyGe_3$-type), $DyGe_{1.85}$ ($DyGe_{1.85}$-type), Dy_3Ge_5 (Y_3Ge_5-type), $DyGe_{1.5}$ (AlB_2-type), Dy_3Ge_4 (Er_3Ge_4-type), DyGe (TlJ-type), $Dy_{11}Ge_{10}$ ($Ho_{11}Ge_{10}$-type), Dy_5Ge_4 (Sm_5Ge_4-type), and Dy_5Ge_3 (Mn_5Si_3-type).

To study the phase equilibria of the Dy–Cr–Ge ternary system, produced alloys were examined by X-ray diffractometry and energy dispersive X-ray spectroscopy. Based on the performed analysis, the isothermal section of the Dy–Cr–Ge system at 1073 K was constructed over the whole concentration range (Fig. 1). The Phase composition of individual alloys is presented in Table 1. Electron micrographs of some samples are shown in Fig. 2.

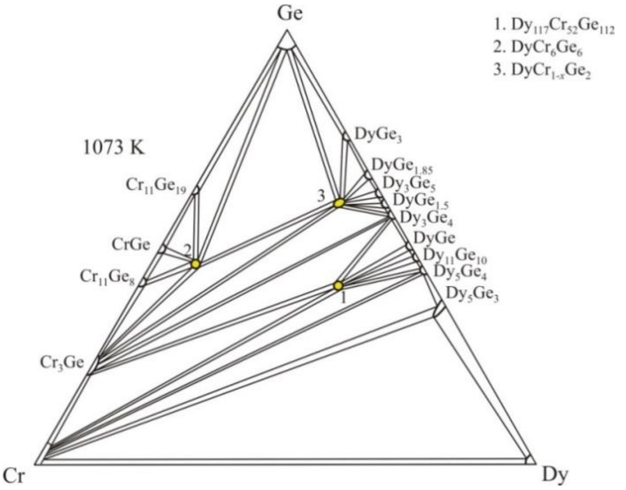

Fig. 1. Isothermal section of the Dy–Cr–Ge system at 1073 K.

At a temperature of 1073 K in the Dy–Cr–Ge system, the formation of two ternary compounds, $DyCr_6Ge_6$ and $DyCr_{1-x}Ge_2$, was confirmed, and the formation of a new compound, $Dy_{117}Cr_{52}Ge_{112}$, was identified. Analysis of the powder pattern of the sample with corresponding composition and the calculated lattice parameter (a = 2.8723(8) nm) indicated that the compound belongs to the $Tb_{117}Fe_{52}Ge_{112}$ (space group $Fm\text{–}3m$) structure type. Crystallographic characteristics of the ternary compounds from the Dy-Cr-Ge system are given in Table 2.

The solubility of Dy, Cr, and Ge in the binary compounds, except for Dy_5Ge_3, may be considered negligible (~1-2.5 at. %). The solubility of Cr in the Dy_5Ge_3 binary germanide extends up to 4 at. % (a = 0.8416(2), c = 0.6261(5) nm for Dy_5Ge_3; a = 0.8432(2), c = 0.6288(2) nm for $Dy_{63}Cr_4Ge_{33}$ sample).

According to the data of the X-ray phase analysis, the $DyCr_{1-x}Ge_2$ compound ($CeNiSi_2$-type) is characterized by a small homogeneity range (x=0.7-0.72), which also includes the $DyCr_{0.3}Ge_2$ composition reported in Ref. [6]. The crystal structure was calculated for the sample $Dy_{31}Cr_9Ge_{60}$ (Fig. 3). Experimental details and refined atomic parameters are given in Tables 3, 4.

A detailed crystal structure study of the $DyCr_6Ge_6$ compound was reported in our recent manuscript [7]. It was found that the $DyCr_6Ge_6$ germanide crystallizes in the $SmMn_6Sn_6$ structure type, a disordered variant of the

Table 1.

Phase composition and EPMA data for individual samples of the Dy–Cr–Ge system

Composition, at. %	Phase	Structure type	Lattice parameters, nm			EPMA data, at. %		
			a	*b*	*c*	Dy	Cr	Ge
$Dy_{30}Cr_{50}Ge_{20}$	Dy_5Ge_3	Mn_5Si_3	0.8424(3)		0.6273(4)			
	Dy_5Ge_4	Sm_5Ge_4	0.7586(3)	1.4563(5)	0.7676(4)			
	(Cr)	(W)	0.2892(3)					
$Dy_{60}Cr_{12}Ge_{28}$ $Dy_{58,57}Cr_{11,10}Ge_{30,33}$	Dy_5Ge_3	Mn_5Si_3	0.8431(3)		0.6291(3)	62.51	3.78	33.71
	(Dy)	Mg	0.3592(3)		0.5654(3)	100.0		
	(Cr)	W	traces				100.0	
$Dy_{15}Cr_{55}Ge_{30}$	Dy_3Ge_4	Gd_3Ge_4	0.4057(2)	1.0637(4)	1.4197(4)			
	Cr_3Ge	Cr_3Si	0.4627(3)					
	$Dy_{117}Cr_{52}Ge_{112}$	$Tb_{117}Fe_{52}Ge_{112}$	2.8724(6)					
$Dy_{40}Cr_{25}Ge_{35}$ $Dy_{42.43}Cr_{33.53}Ge_{35.04}$	Dy_5Ge_4	Sm_5Ge_4	0.7588(3)	1.4543(4)	0.7678(4)	54.31	1.44	44.25
	$Dy_{117}Cr_{52}Ge_{112}$	$Tb_{117}Fe_{52}Ge_{112}$	2.8724(7)			42.76	18.16	39.08
	(Cr)	(W)	0.2893(4)				100.0	
$Dy_{10}Cr_{50}Ge_{40}$ $Dy_{10.18}Cr_{53.36}Ge_{36.46}$	$DyCr_6Ge_6$	$SmMn_6Sn_6$	0,5162(2)		0,8274(4)	7.99	46.55	45.46
	$DyCr_{1-x}Ge_2$	$CeNiSi_2$	0.4139(3)	1.5900(7)	0.4001(1)	30.37	10.07	59.56
	Cr_3Ge	Cr_3Si	0.4625(3)			0.29	77.86	21.85
$Dy_{15}Cr_{40}Ge_{45}$ $Dy_{15.47}Cr_{39.66}Ge_{44.87}$	$DyCr_xGe_2$	$CeNiSi_2$	0.4139(3)	1.5893(6)	0.4001(2)	30.22	9.67	60.11
	Cr_3Ge	Cr_3Si	0.4626(3)			2.09	72.84	25.07
	Dy_3Ge_4	Gd_3Ge_4	0.4055(3)	1.0638(4)	1.4197(5)	42.61	0.08	57.31
$Dy_{45}Cr_{10}Ge_{45}$ $Dy_{45.13}Cr_{11.21}Ge_{43.66}$	DyGe	TlI	0.4251(3)	1.0625(6)	0.3926(4)	51.44	0.15	48.41
	$Dy_{11}Ge_{10}$	$Ho_{11}Ge_{10}$	1.0869(4)		1.6351(5)	55.75	0.91	43.34
	$Dy_{117}Cr_{52}Ge_{112}$	$Tb_{117}Fe_{52}Ge_{112}$	2,8723(3)			41.99	21.18	36.82
$Dy_7Cr_{46}Ge_{47}$ $Dy_{7.23}Cr_{45.53}Ge_{47.24}$	$DyCr_6Ge_6$	$SmMn_6Sn_6$	0.5164(2)		0.8277(2)	8.27	46.08	45.65
	CrGe	FeSi	0.4796(3)				50.42	49.58
$Dy_{40}Cr_{10}Ge_{50}$ $Dy_{40.66}Cr_{11.21}Ge_{48.13}$	Dy_3Ge_4	Gd_3Ge_4	0.4056(2)	1.0638(4)	1.4197(4)	42.22	0.07	57.71
	Cr_3Ge	Cr_3Si	0.4628(3)			2.32	72.81	24.87
	$Dy_{117}Cr_{52}Ge_{112}$	$Tb_{117}Fe_{52}Ge_{112}$	2.8722(4)			41.22	21.36	37.42
$Dy_{10}Cr_{40}Ge_{50}$ $Dy_{9,19}Cr_{42,76}Ge_{48,05}$	$DyCr_6Ge_6$	$SmMn_6Sn_6$	0.5164(3)		0.8276(4)	8.26	46.16	45.58
	$DyCr_{1-x}Ge_2$	$CeNiSi_2$	0.4136(2)	1.5890(6)	0.4001(1)	30,43	9,40	60,17
	(Ge)	C	0.5646(3)			0.45	0.43	99.12
$Dy_{38}Cr_7Ge_{55}$ $Dy_{39.11}Cr_{6.63}Ge_{54.26}$	$DyCr_xGe_2$	$CeNiSi_2$	0.4138(3)	1.5887(6)	0.4001(3)	32.07	9.01	59.92
	Dy_3Ge_4	Gd_3Ge_4	0.4054(3)	1.0638(5)	1.4196(4)	43.05	0.56	56.39
	Cr_3Ge	Cr_3Si	0.4625(4)			1.98	73.06	24.96
$Dy_{35}Cr_5Ge_{60}$	$DyCr_{1-x}Ge_2$	$CeNiSi_2$	0.4133(3)	1.5889(6)	0.4001(2)			
	Dy_3Ge_4	Gd_3Ge_4	0.4057(2)	1.0639(5)	1.4195(4)			
	$DyGe_{1,5}$	AlB_2	0.3907(4)		0.4109(4)			
$Dy_{20}Cr_{15}Ge_{65}$ $Dy_{18.73}Cr_{16.12}Ge_{65,15}$	$DyCr_6Ge_6$	$SmMn_6Sn_6$	0.5163(2)		0.8275(4)	8.52	46.10	45.38
	$DyCr_{1-x}Ge_2$	$CeNiSi_2$	0.4138(4)	1.5886(3)	0.3999(4)	30.45	9.75	59.80
	(Ge)	C	0.5648(3)			0.33		99.67

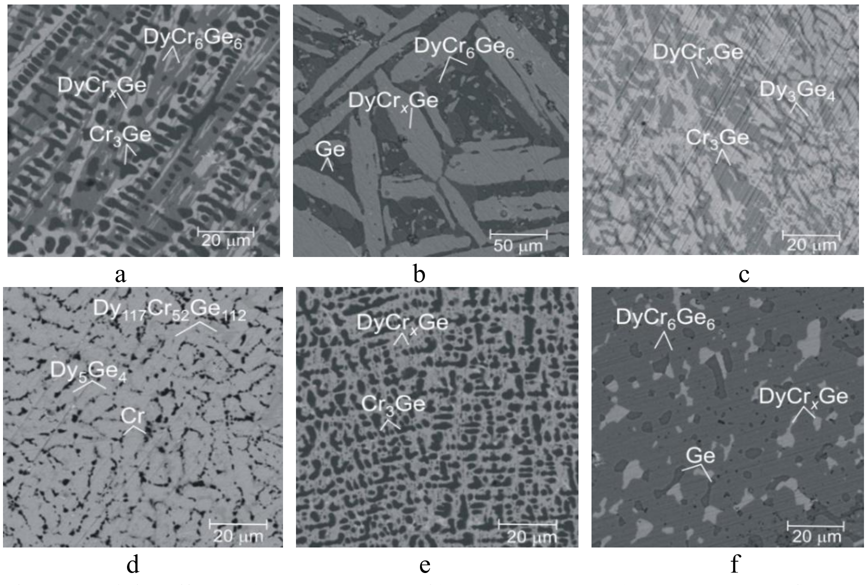

Fig. 2. SEM-images of the alloys: a) $Dy_{10}Cr_{50}Ge_{40}$; b) $Dy_{20}Cr_{15}Ge_{65}$; c) $Dy_{38}Cr_7Ge_{55}$; d) $Dy_{40}Cr_{25}Ge_{35}$; e) $Dy_{15}Cr_{45}Ge_{40}$; f) $Dy_{10}Cr_{40}Ge_{50}$.

Table 2.

Crystallographic characteristics of the ternary compounds from the Dy−Cr−Ge system

Compound	Space group	Structure type	Lattice parameters, nm		
			a	*b*	*c*
$DyCr_6Ge_6$	*P*6/*mmm*	$SmMn_6Sn_6$	0.51642(1)		0.82767(2)
$DyCr_{1-x}Ge_2$	*Cmcm*	$CeNiSi_2$	0.41249(5)- 0.4140(3)	1.5828(2)- 1.5890(7)	0.40048(5)- 0.4001(2)
$Dy_{117}Cr_{52}Ge_{112}$	*Fm*-3*m*	$Tb_{117}Fe_{52}Ge_{112}$	2.8723(8)		

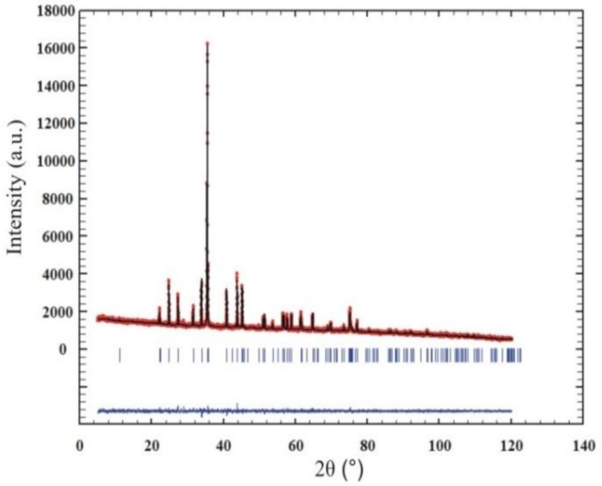

Fig. 3. Experimental (circles), calculated (line) and difference (bottom line) X-ray patterns of the alloy $Dy_{31}Cr_9Ge_{60}$.

$MgFe_6Ge_6$-type. The experimental study that was performed was also confirmed by DFT modeling. These data agree with previous investigations of the isotypic RCr_6Ge_6 compound (R = Ho, Er, Y) studied by neutron diffraction [9].

2.2. DFT modeling

The DFT modeling was performed for the hypothetical $DyCr_xGe_2$ solid solution ($0 \leq x \leq 1$), which includes the experimentally observed ternary $DyCr_{0.28}Ge_2$ compound. The symmetry of the crystal structure was reduced to introduce intermediate compositions (x = 0.25, 0.5, and 0.75). After geometry optimization, the corresponding enthalpies of mixing and formation were calculated, revealing that the formation of the continuous $DyCr_xGe_2$ solid solution ($0 \leq x \leq 1$) is energetically unfavorable (Fig. 4a). Despite the enthalpy of formation becomes less negative with increasing Cr content, the common tangent lines between $DyGe_2$ and $DyCr_6Ge_6$ (ΔH_f = -199 meV/atom [7]) reveal that the most stable composition is ~$DyCr_{0.4}Ge_2$ with a narrow ($0.4 \leq x \leq 0.45$) homogeneity region and two-phase regions towards the $DyGe_2$ and $DyCr_6Ge_6$ compounds.

The distribution of the density of electronic states of $DyCr_{0.25}Ge_2$ (Fig. 4b) predicts its metallic behavior with the valence band formed predominantly by the *s*- and *p*-states of Ge and *d*-states of Cr. The Dy atoms contribute mainly to the density of states above the Fermi level (E_F).

Table 3.

Experimental details and crystallographic data for $DyCr_{0.28}Ge_2$ compound

Alloy composition	$Dy_{31}Cr_9Ge_{60}$
Refined composition	$DyCr_{0.28(5)}Ge_2$
Structure type	$CeNiSi_2$
Pearson symbol	*oS*16
Space group, Z	*Cmcm*; 4
Unit cell parameters: *a*, nm *b*, nm *c*, nm	 0.41249(7) 1.58287(2) 0.40048(5)
Cell volume *V*, nm^3	0.2615(1)
Calculated density D_x, g/cm^3	8.181
Diffractometer	STOE STADI P
Radiation, wavelength λ (nm)	Cu K_α, 1.54056
Angular range / increment (°2θ)	5.000≤2θ≤120.185/0.015
Reliability factors R_{Bragg}, R_f	0.0439, 0.0551

Table 4.

Atomic coordinates and isotropic displacement parameters for $DyCr_{0.28}Ge_2$

Атом	ПСТ	*x*	*y*	*z*	Occupancy	B_{iso}, Å^2
Dy	4*c*	0	0.1036(2)	1/4	1	0.14(9)
Cr	4*c*	0	0.3048(9)	1/4	0.28(5)	1.52(1)
Ge1	4*c*	0	0.0506(7)	1/4	1	1.19(3)
Ge2	4*c*	0	0.7514(6)	1/4	1	1.79(3)

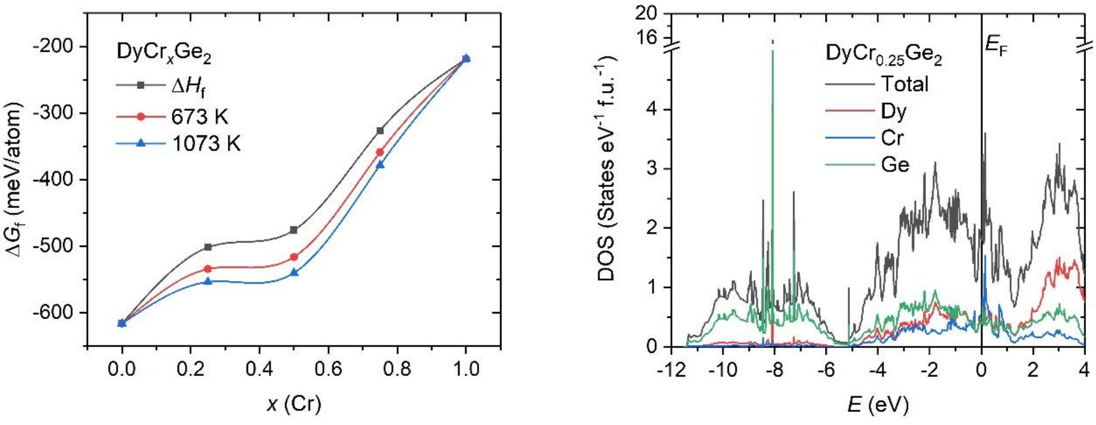

a b

Fig. 4. Calculated energy of formation (ΔG_f) of the hypothetical solid solution $DyCr_xGe_2$ (a) and the distribution of the density of electronic states (DOS) (b) of $DyCr_{0.25}Ge_2$.

The calculated elastic properties of the $DyCr_xGe_2$ solid solution showed that the crystal structure of $DyCrGe_2$ is mechanically unstable. With the increasing Cr content, the bulk (*B*), Yung's (*E*), and shear (*G*) moduli change from 73.3, 106.2, and 42.2 GPa to 84.7, 64.0, and 23.3 GPa, respectively. Meanwhile, the Poisson's ratio increases from 0.259 ($x = 0$) to 0.374 ($x = 0.75$). Increasing Cr content leads to the almost linear rise of Pugh's B/G ratio from 1.738 to 3.638, indicating stronger ductile behavior and lower hardness. The corresponding Debye temperature decreases from 273.7 K ($x = 0$) to 215.2 K ($x = 0.75$).

Conclusions

An experimental study of the interaction of the components in the ternary system Dy–Cr–Ge in the whole concentration range at a temperature of 1073 K has confirmed the existence of ternary germanides $DyCr_6Ge_6$ and $DyCr_{1-x}Ge_2$ and the formation of a new ternary compound $Dy_{117}Cr_{52}Ge_{112}$ with a cubic structure of the $Tb_{117}Fe_{52}Ge_{112}$ type was established. Structural studies of the $DyCr_6Ge_6$ compound proved that it belongs to the $SmMn_6Sn_6$ structure type, a partially disordered variant of the $MgFe_6Ge_6$-type. It was established that the $DyCr_6Ge_6$ and $Dy_{117}Cr_{52}Ge_{112}$ compounds are characterized by a point composition, germanide $DyCr_{1-x}Ge_2$ with $CeNiSi_2$ structure type is characterized by a small homogeneity range, which is limited by the compositions $DyCr_{0.28}Ge_2$ and $DyCr_{0.30}Ge_2$. Solubility of Cr in the Dy_5Ge_3 binary (Mn_5Si_3 structure type) extends up to 4 at. % of Cr. The calculated distribution of the density of electronic states of $DyCr_{0.25}Ge_2$ predicts its metallic behavior with the valence band formed predominantly by the *s*- and *p*-states of Ge and *d*-states of Cr. The thermodynamic modeling showed that the formation of the continuous $DyCr_xGe_2$ solid solution ($0 \le x \le 1$) is energetically unfavorable, which is confirmed by the calculated elastic properties, and that the most stable composition is ~$DyCr_{0.4}Ge_2$ with a narrow ($0.4 \le x \le 0.45$) homogeneity region and two-phase regions towards the $DyGe_2$ and $DyCr_6Ge_6$ compounds.

Acknowledgments

The work was carried out within the framework of the Ministry of Education of Ukraine (grant No 0124U000989). Authors Romaka L., Stadnyk Yu., Konyk M. also thank the Simons Foundation (SFI-PD-Ukraine-00014574) for financial support. The authors thank U. Nitzsche for technical assistance in running DFT calculations on the ITF/IFW computer cluster. V.V.R. is funded by the DFG (project-id 463049368).

Romaka Lyubov – Ph.D., Senior Researcher, Ivan Franko National University of Lviv;
Stadnyk Yuriy – Ph.D., Senior Researcher, Ivan Franko National University of Lviv;
Romaka Vitaliy – D.Sc., doctor of material science, Technische Universität Dresden, Germany;
Yatskiv Yuriy – student, Ivan Franko National University of Lviv;
Konyk Mariya – Ph.D., Senior Researcher, Ivan Franko National University of Lviv.

[1] P.S. Salamakha, Y.M. Prots, *The neodymium-(vanadium, chromium, manganese)-germanium systems*, J. Alloys Compd. 215, 51 (1994); https://doi.org/10.1016/0925-8388(94)90817-6.

[2] M. Konyk, L. Romaka, L. Orovčik, V.V. Romaka, Yu. Stadnyk, *Y−Cr−Ge ternary system at 1070 K*, Visnyk Lviv. Univ. Ser. Chem. 60(1), 38 (2019); https://doi.org/10.30970/vch.6001.038.

[3] M. Konyk, L. Romaka, Yu. Stadnyk, V.V. Romaka, R. Serkiz, A. Horyn, *Er−Cr−Ge ternary system*, Phys. Chem. Solid State. 20(4), 376 (2019); https://doi.org/10.15330/pcss.20.4.376-383.

[4] M. Konyk, L. Romaka, Yu. Stadnyk, V.V. Romaka, V. Pashkevych, *Phase equilibria in the Gd−Cr−Ge system at 1070 K*, Phys. Chem. Solid State. 22(2), 248 (2021); https://doi.org/10.15330/pcss.22.2.248-254.

[5] L. Romaka, Yu. Stadnyk, V.V. Romaka, M. Konyk, *Interaction between the components in Tm−Cr−Ge system at 1070 K*, Phys. Chem. Solid State. 23(4), 633 (2022); https://doi.org/10.15330/pcss.23.4.633-639.

[6] H. Bie, A. Tkachuk, A. Mar, *Structure and magnetic properties of rare-earth chromium germanides* $RECr_xGe_2$ *(RE=Sm,Gd−Er),* J. Solid State Chem. 182, 122 (2009); https://doi.org/10.1016/j.jssc.2008.10.013.

[7] V.V. Romaka, L. Romaka, M. Konyk, L. T. Corredor, K. Srowik, B. Kuzhel, Yu. Stadnyk, Yu. Yatskiv, *Structure, bonding, and properties of* RCr_6Ge_6 *intermetallics (R = Gd-Lu)*, J. Solid State Chem. 338, 124874 (2024); https://doi.org/10.1016/j.jssc.2024.124874.

[8] H. Bie, O.Y. Zelinska, A.V. Tkachuk, A. Mar, *Structures and physical properties of rare-earth chromium germanides* $RECrGe_3$ *(RE= La-Nd, Sm)*, Chem. Mater. 19, 4163 (2007); https://doi.org/10.1021/cm071276.

[9] P. Schobinger-Papamantellos, J. Rodriguez-Carvajal, K.H.J. Buschow, *Ferrimagnetism and disorder in the* RCr_6Ge_6 *compounds (R=Dy, Ho, Er, Y): A neutron study*, J. Alloys Compd. 256, 92 (1997); https://doi.org/10.1016/S0925-8388(96)03109-X.

[10] P. Schobinger-Papamantellos, J. Rodríguez-Carvajal, K.H.J. Buschow, *Atomic disorder and canted ferrimagnetism in the* $TbCr_6Ge_6$ *compound. A neutron study,* J. Alloys Compd. 255, 67 (1997); https://doi.org/10.1016/S0925-8388(96)02872-1.

[11] P.S. Salamakha, Y.M. Prots, *The neodymium-(vanadium, chromium, manganese)-germanium systems*, J. Alloys Compd. 215, 51 (1994); https://doi.org/10.1016/0925-8388(94)90817-6.

[12] A.V. Morozkin, Y.D. Seropegin, V.K. Portnov, I.A. Sviridov, A.V. Leonov, *New ternary compounds* $R_{117}Fe_{52}Ge_{112}$ *(R= Gd, Dy, Ho, Er, Tm) and* $Sm_{117}Cr_{52}Ge_{112}$ *of the* $Tb_{117}Fe_{52}Ge_{112}$*-type structure*, Mater. Res. Bull. 33, 903 (1998); https://doi.org/10.1016/S0025-5408(98)00051-8.

[13] W. Kraus, G. Nolze, *POWDER CELL – a program for the representation and manipulation of crystal structures and calculation of the resulting X-ray powder patterns*, J. Appl. Crystallogr. 29, 301 (1996); https://doi.org/10.1107/S0021889895014920.

[14] T. Roisnel, J. Rodriguez-Carvajal, *WinPLOTR: a Windows tool for powder diffraction patterns analysis*, Mater. Sci. Forum, 378–381, 118 (2001); https://doi.org/10.4028/www.scientific.net/MSF.378-381.118.

[15] G. Kresse, D. Joubert, *From ultrasoft pseudopotentials to the projector augmented-wave method*, Phys. Rev. B 59, 1758 (1999); http://dx.doi.org/10.1103/PhysRevB.59.1758.

[16] J.P. Perdew, K. Burke, M. Ernzerhof, *Generalized gradient approximation made simple*, Phys. Rev. Lett. 77(18), 3865 (1996); https://doi.org/10.1103/PhysRevLett.77.3865.

[17] H. J. Monkhorst, J. K. Pack, *Special points for Brillouin-zone integrations*, Phys. Rev. B 13, 5188 (1976); http://dx.doi.org/10.1103/PhysRevB.13.5188.

[18] G. Henkelman, A. Arnaldsson, H. Jónsson, *A fast and robust algorithm for Bader decomposition of charge density,* Comput. Mater. Sci. 36, 354 (2006); https://doi.org/10.1016/j.commatsci.2005.04.010.

[19] T.B. Massalski in: Binary Alloy Phase Diagrams, ASM, Metals Park, Ohio (1990).

[20] H. Okamoto Desk Handbook: Phase Diagrams for Binary Alloys, Materials Park (OH): American Society for Metals (2000).

Л. Ромака[1], Ю. Стадник[1], В.В. Ромака[2,3], Ю. Яцків[1], М. Коник[1]

Ізотермічний переріз діаграми стану системи Dy–Cr–Ge при 1073 К

[1]*Львівський національний університет імені Івана Франка, Львів, Україна,*
lyubov.romaka@gmail.com
[2]*Технічний Університет м. Дрезден, кафедра неорганічної хімії II, Дрезден, Німеччина,*
vitaliy.romaka@tu-dresden.de
[3]*Інститут дослідження твердого тіла ім. Лейбніца, Дрезден, Німеччина*

Методами рентгенофазового, рентгеноструктурного і рентгеноспектрального аналізів досліджено взаємодію компонентів та побудовано ізотермічний переріз діаграми стану потрійної системи Dy–Cr–Ge при 1073 К у повному концентраційному інтервалі. У системі Dy–Cr–Ge за температури відпалювання утворюються три тернарні сполуки: $Dy_{117}Cr_{52}Ge_{112}$ (структурний тип $Tb_{117}Fe_{52}Ge_{112}$, просторова група *Fm-*3*m*, *a* = 2,8723(8) нм), $DyCr_6Ge_6$ (структурний тип $SmMn_6Sn_6$, просторова група *P*6/*mmm*, *a* = 0,51642(1), *c* = 0,82767(2) нм), $DyCr_{1-x}Ge_2$ (структурний тип $CeNiSi_2$, просторова група *Cmcm*, *a* = 0,41249(5)-0,4140(3), *b* = 1,5828(2)-1,5890(7), *c* = 0,40048(5)-0,4001(2) нм). Сполука $DyCr_{1-x}Ge_2$ характеризується областю гомогенності, яка обмежена складами $DyCr_{0,28}Ge_2$ і $DyCr_{0,30}Ge_2$. Помітною розчинністю третього компонента характеризується ґерманід Dy_5Ge_3 (структурний тип Mn_5Si_3), який розчиняє до 4 ат. % хрому. DFT розрахунки виконано для оцінки еластичних і електричних властивостей сполуки $DyCr_xGe_2$.

Ключові слова: Інтерметалід; рентгенівська дифракція, фазові рівноваги, кристалічна структура.